



# Targeting Multidrug-Resistant *Acinetobacter* spp.: Sulbactam and the Diazabicyclooctenone $\beta$ -Lactamase Inhibitor ETX2514 as a Novel Therapeutic Agent

Melissa D. Barnes,<sup>a,b</sup>  Vijay Kumar,<sup>c</sup> Christopher R. Bethel,<sup>a</sup> Samir H. Moussa,<sup>g</sup> John O'Donnell,<sup>g</sup> Joseph D. Rutter,<sup>a</sup> Caryn E. Good,<sup>h</sup> Kristine M. Hujer,<sup>a,b</sup> Andrea M. Hujer,<sup>a,b</sup> Steve H. Marshall,<sup>a</sup> Barry N. Kreiswirth,<sup>i</sup> Sandra S. Richter,<sup>j</sup> Philip N. Rather,<sup>k,l</sup> Michael R. Jacobs,<sup>b,h</sup>  Krisztina M. Papp-Wallace,<sup>a,b,c</sup> Focco van den Akker,<sup>c</sup> Robert A. Bonomo<sup>a,b,c,d,e,f,m,n</sup>

<sup>a</sup>Louis Stokes Cleveland Veterans Affairs Medical Center Research Service, Cleveland, Ohio, USA

<sup>b</sup>Department of Medicine, Case Western Reserve University, Cleveland, Ohio, USA

<sup>c</sup>Department of Biochemistry, Case Western Reserve University, Cleveland, Ohio, USA

<sup>d</sup>Department of Molecular Biology and Microbiology, Case Western Reserve University, Cleveland, Ohio, USA

<sup>e</sup>Department of Pharmacology, Case Western Reserve University, Cleveland, Ohio, USA

<sup>f</sup>Department of Proteomics and Bioinformatics, Case Western Reserve University, Cleveland, Ohio, USA

<sup>g</sup>Entasis Therapeutics, Waltham, Massachusetts, USA

<sup>h</sup>Department of Pathology, University Hospitals, Cleveland Medical Center, Cleveland, Ohio, USA

<sup>i</sup>Public Health Research Institute Tuberculosis Center, New Jersey Medical School, Rutgers University, Newark, New Jersey, USA

<sup>j</sup>Cleveland Clinic Foundation, Cleveland, Ohio, USA

<sup>k</sup>Department of Microbiology and Immunology, Emory University School of Medicine, Atlanta, Georgia, USA

<sup>l</sup>Research Service, Atlanta Veterans Affairs Medical Center, Decatur, Georgia, USA

<sup>m</sup>CWRU-Cleveland VAMC Center for Antimicrobial Resistance and Epidemiology (Case VA CARES), Cleveland, Ohio, USA

<sup>n</sup>Geriatric Research Education and Clinical Centers (GRECC), Louis Stokes Cleveland Department of Veterans Affairs, Cleveland, Ohio, USA

**ABSTRACT** Multidrug-resistant (MDR) *Acinetobacter* spp. poses a significant therapeutic challenge in part due to the presence of chromosomally encoded  $\beta$ -lactamases, including class C *Acinetobacter*-derived cephalosporinases (ADC) and class D oxacillinases (OXA), as well as plasmid-mediated class A  $\beta$ -lactamases. Importantly, OXA-like  $\beta$ -lactamases represent a gap in the spectrum of inhibition by recently approved  $\beta$ -lactamase inhibitors such as avibactam and vaborbactam. ETX2514 is a novel, rationally designed, diazabicyclooctenone inhibitor that effectively targets class A, C, and D  $\beta$ -lactamases. We show that addition of ETX2514 significantly increased the susceptibility of clinical *Acinetobacter baumannii* isolates to sulbactam. AdeB and AdeJ were identified to be key efflux constituents for ETX2514 in *A. baumannii*. The combination of sulbactam and ETX2514 was efficacious against *A. baumannii* carrying *bla*<sub>TEM-1</sub>, *bla*<sub>ADC-82</sub>, *bla*<sub>OXA-23</sub>, and *bla*<sub>OXA-66</sub> in a neutropenic murine thigh infection model. We also show that, *in vitro*, ETX2514 inhibited ADC-7 ( $k_2/K_i$ ,  $1.0 \pm 0.1 \times 10^6 \text{ M}^{-1} \text{ s}^{-1}$ ) and OXA-58 ( $k_2/K_i$ ,  $2.5 \pm 0.3 \times 10^5 \text{ M}^{-1} \text{ s}^{-1}$ ). Cocrystallization of ETX2514 with OXA-24/40 revealed hydrogen bonding interactions between ETX2514 and residues R261, S219, and S128 of OXA-24/40 in addition to a chloride ion occupied in the active site. Further, the C3 methyl group of ETX2514 shifts the position of M223. In conclusion, the sulbactam-ETX2514 combination possesses a broadened inhibitory range to include class D  $\beta$ -lactamases as well as class A and C  $\beta$ -lactamases and is a promising therapeutic candidate for infections caused by MDR *Acinetobacter* spp.

**IMPORTANCE** The number and diversity of  $\beta$ -lactamases are steadily increasing. The emergence of  $\beta$ -lactamases that hydrolyze carbapenems poses a significant threat to our antibiotic armamentarium. The explosion of OXA enzymes that are carbapenem hydrolyzers is a major challenge (carbapenem-hydrolyzing class D [CHD]). An urgent

**Citation** Barnes MD, Kumar V, Bethel CR, Moussa SH, O'Donnell J, Rutter JD, Good CE, Hujer KM, Hujer AM, Marshall SH, Kreiswirth BN, Richter SS, Rather PN, Jacobs MR, Papp-Wallace KM, van den Akker F, Bonomo RA. 2019.

Targeting multidrug-resistant *Acinetobacter* spp.: sulbactam and the diazabicyclooctenone  $\beta$ -lactamase inhibitor ETX2514 as a novel therapeutic agent. *mBio* 10:e00159-19. <https://doi.org/10.1128/mBio.00159-19>.

**Editor** Gerard D. Wright, McMaster University

This is a work of the U.S. Government and is not subject to copyright protection in the United States. Foreign copyrights may apply.

Address correspondence to Focco van den Akker, [fv5@case.edu](mailto:fv5@case.edu), or Robert A. Bonomo, [robert.bonomo@va.gov](mailto:robert.bonomo@va.gov).

M.D.B. and V.K. contributed equally to this work.

**Received** 20 January 2019

**Accepted** 29 January 2019

**Published** 12 March 2019

need exists to discover  $\beta$ -lactamase inhibitors with class D activity. The sulbactam-ETX2514 combination demonstrates the potential to become a treatment regimen of choice for *Acinetobacter* spp. producing class D  $\beta$ -lactamases.

**KEYWORDS** *Acinetobacter*, DBO, diazabicyclooctanone, diazabicyclooctenone, ETX2514, sulbactam,  $\beta$ -lactamase inhibitor, beta-lactamases, beta-lactams

The discovery of ETX2514, a novel diazabicyclooctenone  $\beta$ -lactamase inhibitor that was derived from the diazabicyclooctanone (DBO), avibactam (Fig. 1), represents a major advance for non- $\beta$ -lactam  $\beta$ -lactamase inhibitors (1, 2). ETX2514 effectively inhibits class A and C  $\beta$ -lactamases and a broad range of class D  $\beta$ -lactamases (1, 2), whereas the spectrum of most DBO inhibition had limited potency against class D OXA  $\beta$ -lactamases (e.g., OXA-48). The introduction of avibactam (Fig. 1) (3), the first commercial member of this inhibitor family, allowed successful inhibition of serine carbapenemases (e.g., KPC-2) and most class C cephalosporinases but with limited activity against class D  $\beta$ -lactamases (4). Avibactam inhibits the enterobacterial carbapenemase OXA-48 with a  $k_2/K_i$  value of  $1.4 \pm 0.1 \times 10^3 \text{ M}^{-1} \text{ s}^{-1}$  (4) but is much less effective at inhibiting other known OXA  $\beta$ -lactamases. For example, the  $k_2/K_i$  value for OXA-10 obtained from *Pseudomonas aeruginosa* is  $1.1 \pm 0.1 \times 10^1 \text{ M}^{-1} \text{ s}^{-1}$  (4). Similarly, the related DBO, relebactam, is also not effective at restoring susceptibility to strains carrying most OXA  $\beta$ -lactamases, with the exception of  $bla_{\text{OXA-48}}$  (5–7).

Unlike other members in the DBO family, the structure of WCK 4234 consists of a nitrile R1 group, and its inhibitory activity extends to OXA-23 ( $k_2/K_i$  value of  $1.7 \pm 0.2 \times 10^4 \text{ M}^{-1} \text{ s}^{-1}$ ) and OXA-24/40 ( $k_2/K_i$  value of  $9.6 \pm 1 \times 10^3 \text{ M}^{-1} \text{ s}^{-1}$ ) (8). Notably, the acylation rates of ETX2514 for OXA-23 and OXA-24/40 are in a similar range ( $5$  to  $9 \times 10^3 \text{ M}^{-1} \text{ s}^{-1}$ ) (2). Moreover, a diverse array of OXA  $\beta$ -lactamases (e.g., OXA-23, OXA-24/40, OXA-51, and OXA-58 families) are prevalent resistance determinants in *Acinetobacter* spp. (2, 9).

ETX2514 was rationally designed as a novel and more versatile inhibitor with increased reactivity and improved binding to  $\beta$ -lactamases, resulting from the addition of a double bond between C3 and C4 and a methyl group at the C3 position compared to avibactam (Fig. 1) (2). In addition to class D  $\beta$ -lactamases OXA-10, OXA-23, and OXA-24/40 inhibition ( $k_2/K_i$  values in the range of  $5$  to  $9 \times 10^3 \text{ M}^{-1} \text{ s}^{-1}$ ), ETX2514 inhibits OXA-48 more robustly with an  $8 \pm 2 \times 10^5 \text{ M}^{-1} \text{ s}^{-1} k_2/K_i$  (2). Further, ETX2514 inhibits class A  $\beta$ -lactamases (e.g., TEM-1, CTX-M-15, KPC-2, and SHV-5) and class C  $\beta$ -lactamases (e.g., AmpC and the *Enterobacter cloacae* AmpC, P99) with  $k_2/K_i$  values ranging from  $9 \pm 2 \times 10^5$  to  $1.4 \pm 0.6 \times 10^7 \text{ M}^{-1} \text{ s}^{-1}$  (2). The imipenem-ETX2514 combination is effective against *Enterobacteriaceae* and *P. aeruginosa* (10). Moreover, the sulbactam-ETX2514 combination extends efficacy to *Acinetobacter baumannii* (10, 11).

Carbapenem hydrolyzing OXA-like  $\beta$ -lactamases, including OXA-23-like, OXA-24/40-like, OXA-58-like, and OXA-143-like, have been identified in *A. baumannii* (12, 13). In the present study, we set out to test the susceptibility of a diverse panel of multidrug-resistant (MDR) *A. baumannii* isolates to sulbactam-ETX2514 as well as further biochemically and structurally characterize the ability of ETX2514 to inhibit class C ADC-7 (the AmpC ortholog in *A. baumannii*) and class D OXA-58 chromosomal  $\beta$ -lactamases which are highly prevalent in clinical isolates of *Acinetobacter* spp.

## RESULTS AND DISCUSSION

**Susceptibility testing of *A. baumannii* clinical strains.** Seventy-two well-characterized *A. baumannii* isolates from the Walter Reed Army Medical Center (WRAMC) were tested against sulbactam with and without ETX2514. Previous characterization of the genetic content of these strains revealed that the majority encoded class C ( $bla_{\text{ADC}}$ ) genes (99%) and class D ( $bla_{\text{OXA-69-like}}$ ) genes (97%). Furthermore, 40% of strains carried a class A  $bla_{\text{TEM}}$  gene, and 11% and 12.5% of the isolates carried class D  $bla_{\text{OXA-23-like}}$  and  $bla_{\text{OXA-58-like}}$  genes, respectively (Table 1) (14). Using the MIC breakpoint for ampicillin-

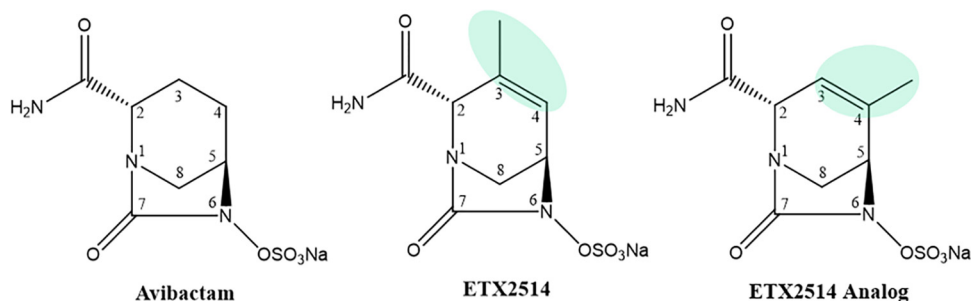


**FIG 1** Structures of the DBOs, avibactam, ETX2514, and ETX2514 analog compound 3.

sulbactam ( $S \leq 8/4$ ;  $I = 16/8$ ,  $R \geq 32/16$  mg/liter) set by the Clinical and Laboratory Standards Institute (CLSI) (15), 47% (34/72) of the isolates were resistant to sulbactam alone ( $MIC \geq 16$  mg/liter), but only one isolate (1%) maintained an MIC higher than 8 mg/liter (i.e., AB054  $MIC = 32$  mg/liter) against sulbactam in combination with 4 mg/liter ETX2514 (Table 2). We rationalized the use of the breakpoint of sulbactam alone taken from the CLSI-defined breakpoints for the ampicillin-sulbactam combination, since ampicillin contributes little activity to sulbactam in *Acinetobacter* spp. (16). Seventeen of the 72 isolates (24%) were resistant to meropenem ( $R \geq 8$  according to CLSI [15]; Table 2).

We also assessed 26 additional *A. baumannii* isolates that were carbapenem resistant ( $R > 8$  mg/liter for meropenem and imipenem) (Table 3): 8 strains were collected from patients at the Brooke Army Medical Center, 10 strains tested were from patients at University Hospitals of Cleveland, and 8 isolates were collected at the Cleveland Clinic Foundation (CCF). ETX2514 combined with sulbactam was also extremely effective against this panel of *A. baumannii* isolates. The addition of ETX2514 lowered the MICs of sulbactam alone by 8- to 64-fold, resulting in MICs of  $\leq 4$  mg/liter for the sulbactam-ETX2514 combination against all 26 strains (Table 3).

The genomic DNA from the four isolates with a sulbactam-ETX2514 MIC of  $\geq 8$  mg/liter was purified for whole-genome sequencing (WGS). All four strains contained a  $bla_{ADC}$  gene (three  $bla_{ADC-25}$  genes and one  $bla_{ADC-79}$  gene),  $bla_{OXA-66}$  (OXA-51-like),  $bla_{TEM-1}$ , and a mutated  $adeJ$  (*Acinetobacter* drug efflux) gene (the homolog of *P. aeruginosa* *mexB*) (Table 4). Strains AB054 and AB070 additionally contained distinct  $pbp3$  mutations. Strain AB070 also carried an additional  $bla_{OXA-69}$  gene (Table 4). Spontaneous resistance to sulbactam-ETX2514 was mapped previously to mutations in the active site of the PBP3 gene, but notably, those mutations and corresponding amino acid substitutions (S395F, S390T, T511S, and V505L) were not identified in these *A. baumannii* isolates (17). The H370Y mutation that was identified in PBP3 (*ftsI* gene) was reported previously and does not seem to contribute to carbapenem resistance (18), but this residue sits at a critical location, at the entrance of the active site, and therefore, could be involved in resistance of other classes of antibiotics. The A578T mutation in the *ftsI* gene is a second

**TABLE 1** Presence of  $\beta$ -lactamase gene in the Walter Reed Army Medical Center (WRAMC) isolates (14)

$\beta$ -Lactamase gene	Prevalence (%) <sup>a</sup>
$bla_{ADC}$	99 (71/72)
$bla_{OXA-69}$ -like	97 (70/72)
$bla_{OXA-23}$ -like	11 (8/72)
$bla_{OXA-58}$ -like	12.5 (9/72)
$bla_{TEM}$	40 (29/72)
$bla_{SHV}$	0 (0/72)
$bla_{PER}$	3 (2/72)

<sup>a</sup>The number of isolates with the  $\beta$ -lactamase gene and total number of isolates are shown within parentheses.

**TABLE 2** Susceptibility of 72 Walter Reed Army Medical Center (WRAMC) *A. baumannii* isolates<sup>a</sup>

Strain	MIC (mg/liter)		
	Sulbactam	Sulbactam-ETX2514 <sup>b</sup>	Meropenem
AB001	16	2	1
AB002	8	1	2
AB003	8	1	2
AB004	4	1	2
AB005	4	1	1
AB006	4	2	4
AB007	4	1	0.5
AB008	4	0.5	1
AB009	4	1	1
AB010	4	1	1
AB011	8	1	1
AB012	4	1	1
AB013	4	1	1
AB014	4	1	1
AB015	4	1	2
AB016	4	1	0.5
AB017	32	1	0.5
AB018	64	1	0.5
AB019	16	1	0.25
AB020	16	1	0.5
AB021	16	1	0.5
AB022	16	1	0.5
AB023	16	1	2
AB024	16	1	0.5
AB025	16	1	0.5
AB026	16	1	1
AB027	16	2	0.5
AB028	16	0.5	0.5
AB029	16	0.5	0.5
AB030	16	0.5	1
AB031	16	0.25	1
AB032	16	0.5	0.5
AB033	64	0.5	1
AB034	16	0.5	1
AB035	16	0.5	0.25
AB036	16	0.5	0.5
AB037	64	0.5	0.25
AB038	16	0.5	1
AB039	4	0.5	1
AB040	32	0.5	0.5
AB041	16	0.5	0.5
AB042	4	0.5	4
AB043	4	1	16
AB044	4	1	8
AB045	2	0.5	8
AB046	4	1	16
AB047	4	1	8
AB048	4	0.5	16
AB049	4	0.5	32
AB050	4	0.5	16
AB051	2	1	1
AB052	64	8	2
AB053	32	8	2
AB054	64	32	32
AB055	16	4	8
AB056	8	1	16
AB057	16	1	32
AB058	32	4	2
AB059	32	1	32
AB060	8	1	32
AB061	8	2	32
AB062	8	2	64
AB063	32	1	0.5

(Continued on next page)

TABLE 2 (Continued)

Strain	MIC (mg/liter)		
	Sulbactam	Sulbactam-ETX2514 <sup>b</sup>	Meropenem
AB064	8	0.5	0.25
AB065	8	2	32
AB066	4	0.5	0.25
AB067	4	0.5	0.25
AB068	4	2	1
AB069	4	1	1
AB070	32	8	2
AB071	8	2	0.5
AB072	4	0.5	0.25
<b>MIC<sub>50</sub></b>	<b>8</b>	<b>1</b>	<b>1</b>
<b>MIC<sub>90</sub></b>	<b>32</b>	<b>2</b>	<b>32</b>

<sup>a</sup>According to CLSI (15), ampicillin-sulbactam  $R \geq 32/16$  mg/liter and meropenem  $R \geq 8$  mg/liter.

<sup>b</sup>The ETX2514 concentration was 4 mg/liter.

shell residue that possibly could affect antibiotic resistance through hydrogen bonding with the addition of the hydroxyl group on the threonine.

A summary of susceptibility profiles for all 98 *A. baumannii* strains tested against sulbactam and sulbactam-ETX2514 is presented in Fig. 2. The MIC<sub>90</sub> of sulbactam against this collection was lowered from 32 mg/liter alone to 2 mg/liter in the presence of 4 mg/liter of ETX2514. These data closely resemble the MIC<sub>90</sub> of 64 mg/liter for sulbactam alone and 4 mg/liter for sulbactam-ETX2514 in a panel of *A. baumannii* isolates in a previous study (2).

**Susceptibility testing of *Acinetobacter* efflux knockout strains.** To further define the contribution of efflux to the antibacterial activity of sulbactam-ETX2514, the MICs of sulbactam with and without ETX2514 against four *A. baumannii* strains and four

TABLE 3 Susceptibility of carbapenem-resistant *A. baumannii* isolates<sup>a</sup>

Strain	MIC (mg/liter)			
	Sulbactam	Sulbactam-ETX2514 <sup>b</sup>	Meropenem	Imipenem
VA-432	16	2	64	32
VA-433	16	1	32	16
VA-434	16	2	64	64
VA-435	16	2	64	32
VA-436	16	2	64	64
VA-437	8	2	32	32
VA-438	8	1	32	16
VA-505	8	1	32	32
UH AB636	16	2	>8	>8
UH AB667	32	4	>8	>8
UH AB477	16	2	>8	>8
UH AB491	16	2	>8	>8
UH AB660	16	2	>8	>8
UH AB202	16	2	>8	>8
UH AB461	8	1	>8	>8
UH AB489	16	1	>8	>8
UH AB487	16	2	>8	>8
UH AB490	16	2	>8	>8
CCF 1MR	32	2	>8	>8
CCF 2MR	16	0.25	>8	>8
CCF 3MR	4	0.5	>8	>8
CCF 4MR	16	1	>8	>8
CCF 5MR	16	2	>8	>8
CCF 6MR	16	2	>8	>8
CCF 7MR	32	4	>8	>8
CCF 8MR	8	0.5	>8	>8

<sup>a</sup>According to CLSI guidelines (15), ampicillin-sulbactam  $R \geq 32/16$  mg/liter, meropenem  $R \geq 8$  mg/liter, and imipenem  $R \geq 8$  mg/liter.

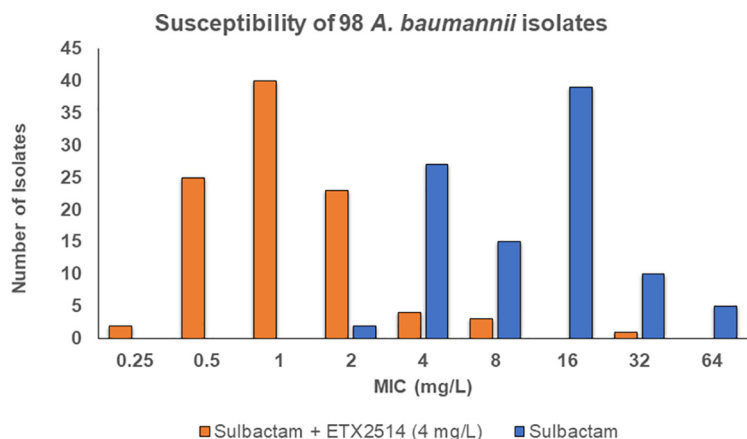
<sup>b</sup>The ETX2514 concentration was 4 mg/liter.

**TABLE 4** Presence of relevant genes ( $\beta$ -lactamases, PBP, and efflux gene mutations) in the four WRAMC isolates with sulbactam-ETX2514 MICs of  $\geq 8$  mg/liter

Strain	Relevant genotype
AB052	<i>bla</i> <sub>ADC-25</sub> + <i>bla</i> <sub>OXA-66</sub> + <i>bla</i> <sub>TEM-1</sub> + <i>adeJ</i> [A326V] +
AB053	<i>bla</i> <sub>ADC-25</sub> + <i>bla</i> <sub>OXA-66</sub> + <i>bla</i> <sub>TEM-1</sub> + <i>adeJ</i> [A326V] +
AB054	<i>bla</i> <sub>ADC-25</sub> + <i>bla</i> <sub>OXA-66</sub> + <i>bla</i> <sub>TEM-1</sub> + <i>adeJ</i> [S1010R] + <i>pbp3</i> [A578T] +
AB070	<i>bla</i> <sub>ADC-79</sub> + <i>bla</i> <sub>OXA-66</sub> + <i>bla</i> <sub>OXA-69</sub> + <i>bla</i> <sub>TEM-1</sub> + <i>adeJ</i> [L670R] + <i>pbp3</i> [H370Y] +

*Acinetobacter nosocomialis* strains with inactivated efflux constituents were compared to the respective wild-type parent of each species. The *A. nosocomialis* M2 strain was isolated from a patient in 1996 in Cleveland, Ohio (19). While the activity of sulbactam did not change upon addition of ETX2514 against any isogenic mutant tested compared to the parent strain, the addition of ETX2514 led to substantial decreases in sulbactam MICs in *A. baumannii* devoid of *adeB* and/or *adeJ* efflux pump genes, suggesting that ETX2514 is a substrate for these pumps (Table 5). These multidrug transporters are components of two out of the three most prevalent efflux pumps in *A. baumannii*, *adeABC*, *adeFGH*, and *adeIJK* (20). *adeABC* was the first resistance-nodulation-division (RND) efflux pump system characterized in *A. baumannii* (21, 22). A study in 2013 found that 10 out of 14 MDR clinical isolates overexpressed the *adeABC* operon, but not the other efflux systems (20). The toxic nature of high levels of *adeIJK* in multidrug-resistant *A. baumannii* predicts that overexpression of *adeABC* would be more prevalent than *adeIJK* in this species (23). In contrast to *A. baumannii*, susceptibility of *A. nosocomialis* strains was mostly affected by loss of the *adeJ* efflux pump (Table 5). Further investigation is needed to determine the relative effect on susceptibility to sulbactam-ETX2514 in *Acinetobacter* spp. overexpressing these efflux determinants.

**Murine thigh infection model of *A. baumannii*.** The *in vivo* efficacy of the sulbactam-ETX2514 combination was evaluated in a neutropenic mouse thigh infection model using *A. baumannii* ARC5955 carrying *bla*<sub>TEM-1</sub>, *bla*<sub>ADC-82</sub>, *bla*<sub>OXA-23</sub>, and *bla*<sub>OXA-66</sub> (OXA-51-like) genes. This strain demonstrates poor susceptibility to sulbactam *in vitro* with an MIC of 64 mg/liter; however, susceptibility is restored in the presence of ETX2514 with a potentiated MIC of 4 mg/liter (24). As shown in Table 6, subcutaneous administration of sulbactam and ETX2514 individually every 3 h at doses of 75 and 50 mg/kg of body weight resulted in  $>2 \log_{10}$  CFU/g of growth in 24 h (vehicle control =  $+3.39 \log_{10}$  CFU/g). In combination at the same doses, however,  $>1$ -log CFU/g of bactericidal activity is realized relative to the CFU burden at the beginning of treatment. Increasing the ETX2514 dose to 200 mg/kg in combination with 50 mg/kg sulbactam resulted in a  $1.5 \log_{10}$  CFU/g reduction, exceeding the performance of colistin ( $-1.36 \log_{10}$  CFU/g), which was used as a positive control for the study.

**FIG 2** Susceptibility summary of 98 *A. baumannii* clinical isolates.

**TABLE 5** Susceptibility of efflux knockouts in *Acinetobacter*

<i>Acinetobacter</i> species (strain)	Efflux knockout	MIC (mg/liter)		Fold change
		Sulbactam	Sulbactam-ETX2514	
<i>A. baumannii</i> (ATCC 17978)	WT	1	1	0
	$\Delta adeB$	1	0.125	8
	$\Delta adeJ$	1	0.125	8
	$\Delta adeB/\Delta adeJ$	1	0.125	8
<i>A. nosocomialis</i> (M2)	WT	2	1	2
	$\Delta adeB$	2	1	2
	$\Delta adeJ$	2	0.125	16
	$\Delta adeB/\Delta adeJ$	2	0.125	16

**Kinetic analysis.** ADC-7 is acylated by ETX2514 very quickly with a rate constant of  $1.0 \pm 0.1 \times 10^6 \text{ M}^{-1} \text{ s}^{-1}$  (Table 7). The acylation rate constant ( $k_2/K_i$ ) of ETX2514 for OXA-58 is appreciable, albeit four times lower than for ADC-7. In addition, the  $k_{\text{off}}$  for ADC-7 ( $8 \pm 1 \times 10^{-4} \text{ s}^{-1}$ ) was fivefold faster than that for OXA-58 ( $1.6 \pm 0.3 \times 10^{-4} \text{ s}^{-1}$ ). Both  $\beta$ -lactamases shared the same  $K_d$  value (1 nM). The partition ratio ( $k_{\text{cat}}/k_{\text{inact}}$ ) (1) was the same for ADC-7 and OXA-58, showing that the  $\beta$ -lactamases do not hydrolyze ETX2514 at an appreciable rate (Table 7). Due to its prevalence in clinical isolates of *A. baumannii*, we also purified and characterized OXA-66 (OXA-51-like). However, sulbactam was found to be a very poor substrate for this enzyme (data not shown), which also was only modestly inhibited by ETX2514 ( $K_{i \text{ app}} 43 \pm 4 \mu\text{M}$ ,  $k_2/K_i 600 \pm 0.7 \text{ M}^{-1} \text{ s}^{-1}$ ).

**Mass spectrometry of the binding of ETX2514 to  $\beta$ -lactamases.** To identify intermediates in the reaction of ETX2514 with ADC-7 and OXA-58, the  $\beta$ -lactamases were incubated with ETX2514 at a 1:1 molar ratio for 5 min, 30 min, and 24 h prior to analysis by mass spectrometry (Fig. 3).

**Timed mass spectrometric analysis of ADC-7.** The ADC-7  $\beta$ -lactamase was detected as a mass of 40,637 Da (Fig. 3). Incubation of ADC-7 with ETX2514 resulted in the expected mass addition of 277 Da ( $40,914 \pm 5 \text{ Da}$ ), consistent with an adduct of the full ETX2514 molecule. A mass corresponding to the net loss of the sulfate group from ETX2514 bound to ADC-7 was also observed as a minor product at  $40,834 \pm 5 \text{ Da}$  ( $40,914 - 80 \text{ Da}$ ). An additional mass at 40,815 Da corresponding to the loss of water from the desulfated acyl complex was determined. Interestingly, the intensity of the peaks corresponding to the desulfated acyl enzyme did not change significantly over 24 h. Desulfation seems to occur selectively for avibactam, but not for the relebactam or zidebactam DBOs, by the class A KPC-2 as was observed previously (4, 8, 25).

**Timed mass spectrometric analysis of OXA-58.** The OXA-58  $\beta$ -lactamase was detected as a mass of 29,232 Da  $\pm 5 \text{ Da}$  (Fig. 3). Incubation of OXA-58 with ETX2514 resulted in the expected mass addition of 277 Da ( $29,509 \text{ Da} \pm 5 \text{ Da}$ ). A mass corresponding to the net loss of the sulfate group from ETX2514 bound to ADC-7 was observed at  $29,428 \text{ Da} \pm 5 \text{ Da}$  ( $29,509 - 79 \text{ Da}$ ). An additional mass at 29,412 Da corresponding to the loss of water from the desulfated acyl complex was noted. The

**TABLE 6** Change in  $\log_{10}$  CFU/g burden in thigh tissue 24 h after initiation of therapy to CD-1 mice

Group ID	Dose (mg/kg)	Route/regimen	$\log_{10}$ CFU/g	SD	Change in $\log_{10}$ CFU/g
T = Rx	n/a	n/a	6.6	0.23	
26-h infection control	Vehicle	SC/q3h	10.0	0.19	3.4
Sulbactam	75	SC/q3h	9.0	0.22	2.5
ETX2514	50	SC/q3h	8.8	0.31	2.2
ETX2514-sulbactam	12.5:75	SC/q3h	6.6	0.49	0.01
ETX2514-sulbactam	50:75	SC/q3h	5.6	0.34	-1.0
ETX2514-sulbactam	200:75	SC/q3h	5.1	0.23	-1.5
Colistin	40	SC/q24h	5.3	0.33	-1.4

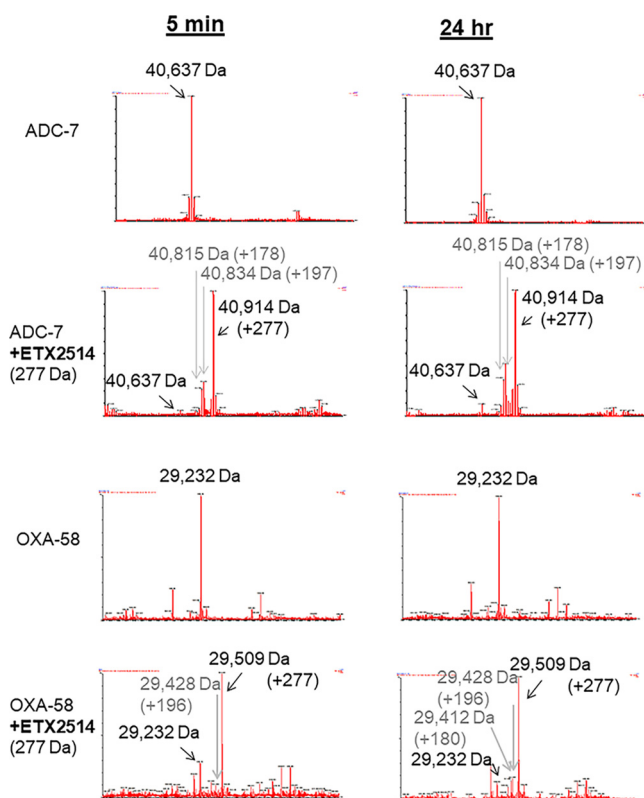
**TABLE 7** Kinetic parameters of  $\beta$ -lactamase inhibition by ETX2514

Drug	$K_{i\text{ app}}$ ( $\mu\text{M}$ )	$k_2/K_i$ ( $\text{M}^{-1} \text{s}^{-1}$ )	$k_{\text{off}}$ (residence time) ( $\text{s}^{-1}$ )	$k_{\text{off}}$ (residence time half-life) (min)	$K_d$ (nM)	$k_{\text{cat}}/k_{\text{inact}}$
ADC-7	$0.11 \pm 0.01$	$1.0 \pm 0.1 \times 10^6$	$8 \pm 1 \times 10^{-4}$	$14 \pm 1$	$1 \pm 0.1$	1
OXA-58	$0.39 \pm 0.04$	$2.5 \pm 0.3 \times 10^5$	$1.6 \pm 0.3 \times 10^{-4}$	$72 \pm 8$	$1 \pm 0.2$	1

mass peaks corresponding to desulfated acyl complex were relatively small and did not dramatically change in intensity after 24 h.

**Mass spectrometry of the ETX2514 acyl transfer between OXA-58 and KPC-2  $\beta$ -lactamases.** To test the reversibility of the ETX2514 binding to OXA-58 and whether ETX2514 binds and dissociates as an intact compound or is modified, the class A KPC-2  $\beta$ -lactamase was used as the acceptor  $\beta$ -lactamase to bind any ETX2514 that dissociated from the acylated OXA-58 (donor  $\beta$ -lactamase). Mass spectra of the reaction showed only the acylated OXA-58 with intact ETX2514 (+277 Da) from 15 s to 24 h (Fig. 4). ETX2514 did not transfer to KPC-2 under these conditions, which is consistent with a previous report of a lack of acyl exchange between ETX2514 acylated-OXA  $\beta$ -lactamases and CTX-M-15 up to 18 h (1). In the single  $\beta$ -lactamase control reaction using KPC-2 incubated with ETX2514, the intact (+277 Da) ETX2514 was detected bound to KPC-2 after a 15-s incubation, but at 24 h, only a mass addition of 197 Da was detected, corresponding to a desulfated ETX2514 (Fig. 4). The detection of desulfated ETX2514 bound to KPC-2 and the slow regeneration of unacylated KPC-2 due to ETX2514 were reported previously (1).

**Crystallography.** Herein is the first crystallization of OXA-24/40 with ETX2514. The crystal structure of the adduct of ETX2514 with a related carbapenem-hydrolyzing class D  $\beta$ -lactamase, OXA-24/40, revealed a well-ordered opened ring product of ETX2514 covalently bound to the catalytic serine S81 (Fig. 5). The K84 residue was observed to

**FIG 3** Mass spectra of ADC-7 and OXA-58  $\beta$ -lactamases and ETX2514. Mass accuracy is within 5 Da.

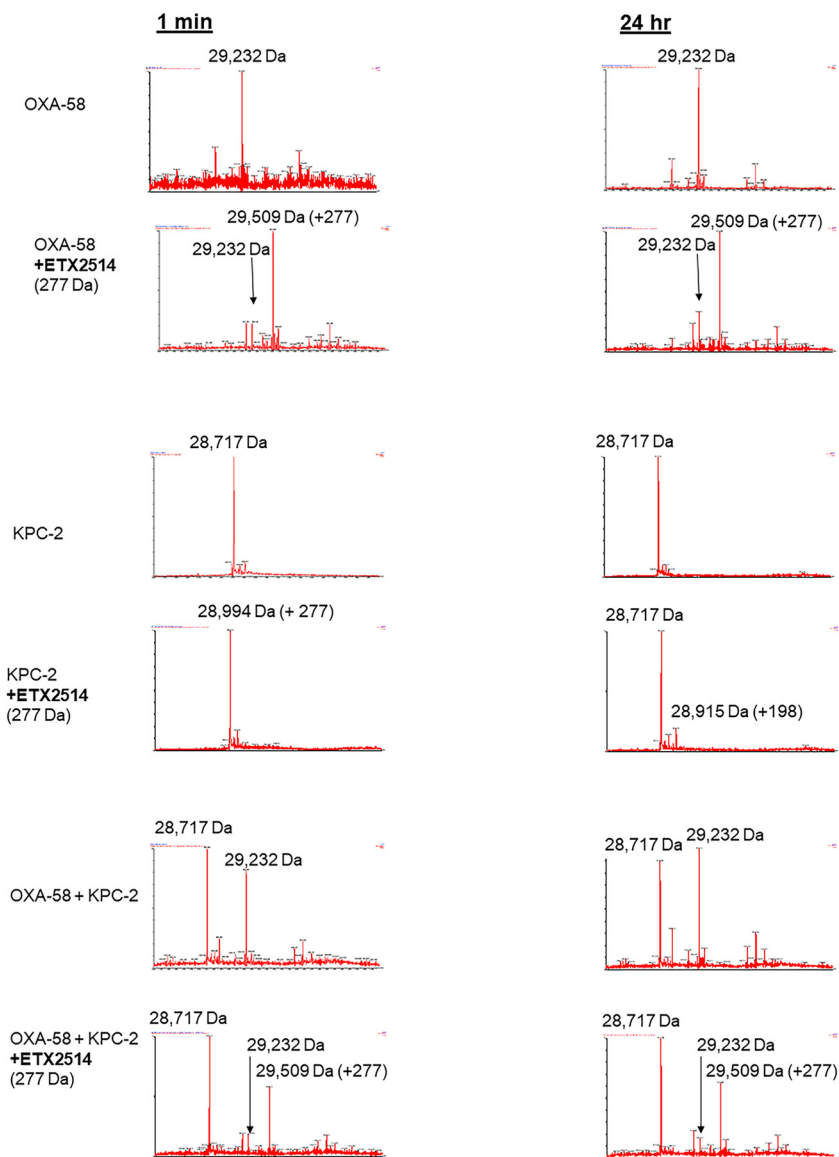


**FIG 4** Mass spectra of ETX2514 acyl transfer from OXA-58 using KPC-2 as the recipient  $\beta$ -lactamase. Mass accuracy is within 5 Da.

be partially carbamylated with an occupancy of 0.6 (Fig. 5); the occupancy of the noncarbamylated K84 side chain was 0.4, and a chloride ion (also 0.4 occupancy) was present instead of the carboxyl moiety. This was not surprising, as the active site lysine residue in OXA-24 has been shown to exist in equilibrium as carboxylated and non-carboxylated species (26). Further, the presence of the chloride ion was previously also observed for a related DBO inhibitor in complex with OXA-24/40 (27). The carbonyl oxygen of ETX2514 occupies the oxyanion hole formed by the backbone nitrogens of S81 and W221. The sulfate moiety of ETX2514 interacts with R261, S219, and S128. The nitrogen atom attached to the sulfate moiety interacts with S128, whereas the nitrogen atom of the amide moiety interacts with the backbone oxygen of W221. The latter direct protein interaction with the amide of ETX2514 was not observed for avibactam when complexed to OXA-24/40 (Fig. 6).

Interestingly, the tetrahydropyridine ring of ETX2514 adopts a chair-like conformation similar to what was observed for avibactam as well as the ETX2514 analog compound 3 (2) (Fig. 1, 6, and 7). The  $IC_{50}$ s of ETX2514 and compound 3 for OXA 24/40 are 0.19  $\mu$ M and 0.36  $\mu$ M, respectively, compared to that of avibactam at 16  $\mu$ M (2). The

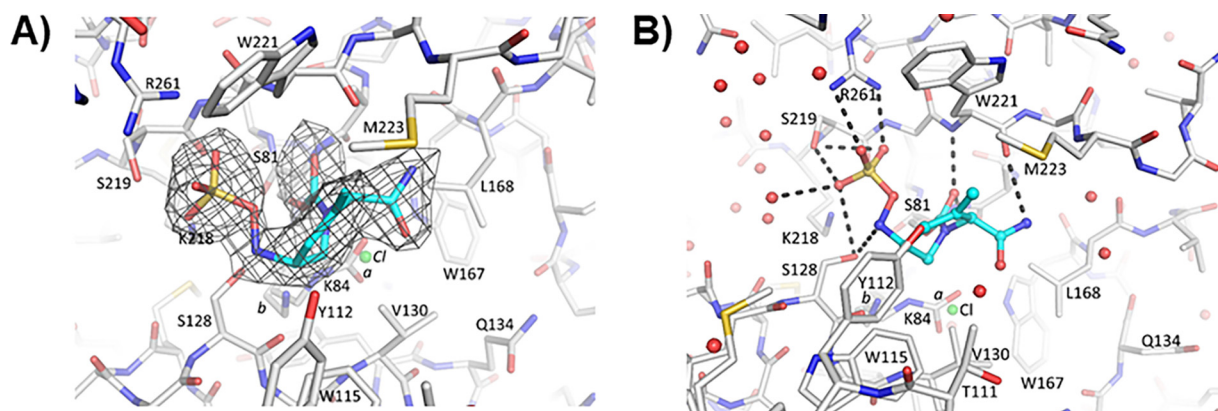


**FIG 5** ETX2514 in the active site of OXA-24/40. (A) Shown is an unbiased omit  $|F_o| - |F_c|$  electron density with ETX2514 removed from refinement and map calculations of OXA-24/40. The inhibitor is shown in blue carbon atom stick representation, whereas the protein is depicted in gray carbon atom stick representation. Electron density is contoured at the  $3\sigma$  level. The K84 side chain was observed in two conformations; one carbamylated and one noncarbamylated (0.6 and 0.4 occupancy conformations labeled *a* and *b*, respectively). A chloride ion with 0.4 occupancy was also refined in the active site (green sphere labeled Cl). (B) Hydrogen bonds (dashed lines) between ETX2514 and OXA-24/40. Water molecules are depicted as red spheres, and the partially occupied chloride ion is depicted as a green sphere.

presence of the extra methyl at the C3 position in ETX2514, compared to compound 3, shifts the side chain of M223 to potentially form tighter van der Waals interactions (Fig. 7). In addition to increasing the chemical reactivity of the DBO core, the double bond in ETX2514, not present in avibactam, gives the six-membered ring in ETX2514 a more planar character to present the C3 methyl group at the right orientation (Fig. 5 and 6). An additional difference between the ETX2514 and avibactam OXA-24/40 crystal structure complexes is the presence of a water molecule near the sulfate of avibactam which was not observed in the ETX2514 complex (“wat1” in Fig. 6). A likely reason for the absence of this water in the ETX2514 complex is that it would be situated at 4.1 Å from the methyl group attached to the C3 ring atom; this environment would probably be too hydrophobic to allow a water molecule to stably cluster at this position in the ETX2514 complex. The possibility of water occupancy differences adjacent to the sulfate of avibactam/ETX2514 in OXA-24/40 complexes was previously also observed in molecular dynamics simulations (2). A water molecule present at this position in close proximity to the ETX2514 sulfate moiety could affect the deacylation rate, and thus

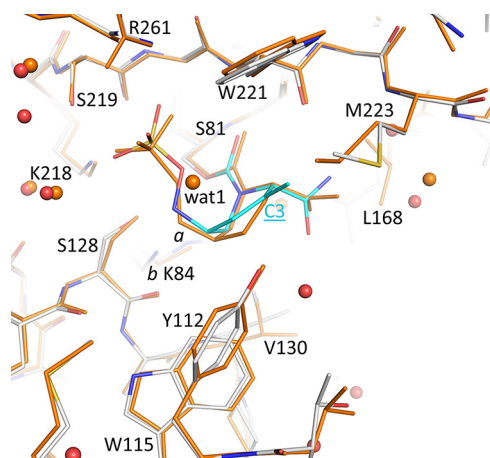


**FIG 6** Superposition of ETX2514 and avibactam OXA-24/40 complexes. The avibactam OXA-24/40 complex (PDB ID 4wm9 [38]) is colored orange; the ETX2514 complex is colored as described in the legend to Fig. 5. The C3 atom for ETX2514 is labeled; the two conformations of K84 are labeled *a* and *b*. Crystallographic water molecules observed in the two structures are shown as spheres (colored red and orange for the ETX2514 and avibactam OXA-24/40 complexes, respectively).

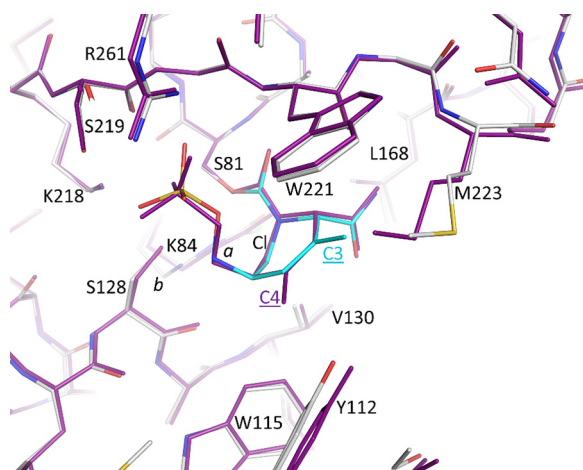


**FIG 7** Superpositioning of ETX2514 and compound 3 OXA-24/40 complexes. The compound 3 OXA-24/40 complex (PDB ID 5vfd [2]) is colored magenta; the ETX2514 complex is colored as in Fig. 5. The differentiating methyl substituents on the DBO ring are labeled C4 (for compound 3) and C3 for ETX2514.

efficacy, since that step involves movement of the sulfate moiety to position its bonded nitrogen atom in close proximity to the carbonyl carbon of the bicyclic ring.

**Conclusions.** In the present study, we show that sulbactam-ETX2514 effectively restores sulbactam susceptibility in *A. baumannii* clinical isolates. Only 4 isolates out of 98 tested against the sulbactam-ETX2514 combination demonstrated an MIC of  $\geq 8$  mg/liter. In addition, sulbactam-ETX2514 demonstrates robust efficacy in a neutropenic thigh model against *A. baumannii* ARC5955, a strain that expresses  $\beta$ -lactamases associated with sulbactam degradation (28). Equivalent exposure of ETX2514 and sulbactam in this murine study has been achieved in first-in-human trials suggesting that the combination has the potential to work therapeutically in a clinical setting. Using whole-genome sequencing, mutations in the *adeJ* efflux pump and/or *pbp3* were identified as potential contributors to the elevated MIC values. Indeed, susceptibility testing of *A. baumannii* isolates lacking individual or a combination of efflux pumps against sulbactam with and without ETX2514 showed increased susceptibility of the strains that were missing *adeB* and/or *adeJ* efflux pumps.

Our findings further show that ETX2514 efficiently inhibits ADC-7 and OXA-58  $\beta$ -lactamases. Inactivation of the class D  $\beta$ -lactamases by a DBO was also recently shown with WCK 4234 that inactivates OXA-23, OXA-24/40, and OXA-51  $\beta$ -lactamases (27). ETX2514 acylates ADC-7 with a rate constant of  $1.0 \pm 0.1 \times 10^6 \text{ M}^{-1} \text{ s}^{-1}$  and deacylates with a rate constant of  $8 \pm 1 \times 10^{-4} \text{ s}^{-1}$ . A small but consistent amount of desulfated acyl complex was observed with ADC-7 and OXA-58. Further, acyl transfer experiments show that ETX2514 does not transfer from acylated OXA-58 to KPC-2. This behavior mimics the interactions of ETX2514 with other OXA  $\beta$ -lactamases (1). Our study is the first to show ETX2514 cocrystallized with OXA-24/40. OXA-24/40 residues R261, S219, and S128 interact with ETX2514 in the active site, and ETX2514 displaces M223. A chloride ion was also identified in the active site in the ETX2514-OXA-24/40 structure. The ability of ETX2514 to efficiently inhibit the class D OXA carbapenemases in addition to the class A and C  $\beta$ -lactamases makes sulbactam-ETX2514 a promising antibiotic combination for the treatment of *Acinetobacter* infections, for which it has recently completed phase 2 clinical testing (ClinicalTrials.gov identifier NCT03445195).

## MATERIALS AND METHODS

**Critical reagents.** ETX2514 powder was provided by Entasis Therapeutics. Sulbactam was purchased from AstaTech. Nitrocefin (catalog no. BR0063G) was purchased from Oxoid.

**Susceptibility testing.** Strains were phenotypically characterized using Mueller-Hinton agar dilution MICs according to the criteria of the CLSI, as previously described (15). A Steer's Replicator was used to obtain MICs using sulbactam, ETX2514, and sulbactam-ETX2514. In testing, the sulbactam concentration

was varied, while ETX2514 was held at a constant concentration of 4 mg/liter. All MIC measurements were performed at least three times, and the mode of the replicates is reported.

For susceptibility testing against carbapenems, MICs were determined by broth microdilution in 96-well plates customized by ThermoFisher Scientific (Cleveland, OH) or TREK Diagnostic Systems (Cleveland, OH), according to CLSI guidelines.

**ADC-7  $\beta$ -lactamase purification.** The ADC-7  $\beta$ -lactamase was purified from *Escherichia coli* BL21(DE3) cells carrying the pET-24a(+)*bla*<sub>ADC-7</sub> plasmid. Cells were grown in super optimal broth (SOB) at 37°C to an approximate optical density at  $\lambda$  600 nm ( $OD_{600}$ ) of 0.6 to 0.8 and induced with 0.5 mM isopropyl- $\beta$ -D-1-thiogalactopyranoside (IPTG) for a minimum of 3 h to express the  $\beta$ -lactamase. The cells were pelleted and frozen at  $-20^{\circ}\text{C}$  for  $\geq 12$  h prior to lysis in 50 mM Tris-HCl buffer, pH 7.4, containing 40 mg/ml lysozyme, 0.1 mM magnesium sulfate, and 250 U benzonase nuclease. The supernatant was further purified by preparative isoelectric focusing (pIEF), eluted from the Sephadex 10 mM phosphate-buffered saline (PBS) at pH 7.4, and polishing steps were completed on a HiLoad 16/600 Superdex 75 pg gel filtration column (GE Healthcare). The final sample of protein was concentrated using centrifugal filter units with a molecular weight cutoff of 10,000 daltons (Millipore). The purity of the protein was assessed by quadrupole time of flight (Q-TOF) mass spectrometry and Coomassie blue-stained SDS-PAGE.

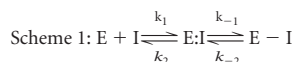
**OXA-24/40  $\beta$ -lactamase purification.** OXA-24/40 was expressed and purified from *E. coli* BL21(DE3) cells expressing *bla*<sub>OXA-24/40</sub> pET24 (+) as previously described (27). Briefly, cells were grown in SOB with 50  $\mu\text{g/ml}$  kanamycin and induced with IPTG. Cells were centrifuged to pellets and frozen at  $-20^{\circ}\text{C}$  at least overnight. Cells were lysed in 50 mM Tris-HCl (pH 7.4) with 40  $\mu\text{g/ml}$  lysozyme, 1 mM  $\text{MgSO}_4$ , and 250 U benzonuclease, and debris was cleared by centrifugation. Lysate was processed by an overnight preparative isoelectric focusing (pIEF), and a nitrocefin was used to identify the region of the  $\beta$ -lactamase. OXA-24/40 eluted from the pIEF was further purified on a HiLoad 16/60 Superdex 75 column (GE Healthcare Life Science).

**OXA-58 and OXA-66  $\beta$ -lactamase purification.** The OXA-58 (H22-L280) and OXA-66 (P27-L274)  $\beta$ -lactamase genes were cloned into pET30a downstream of the *pelB* signal sequence and transformed into *E. coli* Rosetta2 (DE3) pLys5 cells. Cells were grown in 1 liter of LB to an  $OD_{600}$  of approximately 0.6 at 37°C. The culture was cooled in an ice water bath to room temperature and then induced with 0.5 mM isopropyl- $\beta$ -D-1-thiogalactopyranoside (IPTG) for 16 h at 23°C. The cells were pelleted at  $6,000 \times g$  for 30 min, and the pellets were stored at  $-20^{\circ}\text{C}$ . Cell pellets were resuspended in 50 mM 4-(2-hydroxyethyl)-1-piperazineethanesulfonic acid (HEPES) (pH 7) with a protease inhibitor. For OXA-66, DNase and magnesium chloride were also added. Cells were subjected to two rounds of lysis using a French press at 16,000 lb/in<sup>2</sup>, and the lysates were cleared by centrifugation at  $12,000 \times g$  for 20 min.  $\beta$ -Lactamases were purified from the resulting supernatant using a cation exchange column in 50 mM HEPES (pH 7) and eluted by the addition of a linear gradient of sodium chloride of up to 1 M. Further purification of OXA-58 was conducted using a HiLoad 16/600 Superdex 200 gel filtration column preequilibrated with 50 mM HEPES buffer (pH 7) with 100 mM sodium chloride for OXA-58 and 50 mM sodium phosphate (pH 7) for OXA-66. The final stock concentrations of OXA-58 and OXA-66 were 1 mM and 0.12 mM, respectively.

**$\beta$ -Lactamase steady-state kinetic analysis.** Kinetic parameters at 482 nm for nitrocefin and 297 nm for imipenem were determined using an Agilent (Santa Clara, CA) 8453 diode array spectrophotometer using a 1-cm-path-length cuvette. All reactions with ADC-7 were conducted in 10 mM PBS at pH 7.4 at room temperature. Stock solutions of OXA-58 and OXA-66 were diluted accordingly in 50 mM sodium phosphate (pH 7.2). Reactions with OXA-58 and OXA-66 were conducted in 50 mM sodium phosphate (pH 7.2) and 20 mM sodium bicarbonate at ambient temperature.

The  $K_m$  and  $V_{max}$  for ADC-7 and OXA-58  $\beta$ -lactamases and nitrocefin (NCF) were determined by maintaining the enzyme at low nanomolar concentrations and using NCF in excess molar concentration to establish pseudo-first-order kinetics. The resulting data were fit to the Henri Michaelis-Menten equation using Origin 9.1 (OriginLab, Northampton, MA).

The mechanism of inactivation of  $\beta$ -lactamases by ETX2514 is represented according to the following scheme which is based on previous work with  $\beta$ -lactamases and avibactam (3, 29):



**$K_{i \text{ app}}$ .** Determination of  $K_{i \text{ apparent}}$  ( $K_{i \text{ app}}$ ) was described previously (30).  $K_{i \text{ app}}$  was determined for  $\beta$ -lactamases using a direct competition assay under steady-state conditions. ADC-7  $\beta$ -lactamase (0.74 nM) was mixed with 100  $\mu\text{M}$  NCF ( $K_m = 20 \mu\text{M}$ ) and 100 to 400 nM ETX2514, and the reaction velocity was monitored for the first 10 s of the reaction. The reaction velocity of OXA-58  $\beta$ -lactamase (2 nM), 85  $\mu\text{M}$  NCF ( $K_m = 17 \mu\text{M}$ ), and 750 to 2,000 nM ETX2514 was monitored for the first 10 s. OXA-66  $\beta$ -lactamase (380 nM) was mixed with 300  $\mu\text{M}$  imipenem ( $K_m = 60 \mu\text{M}$ ) and 150 to 300  $\mu\text{M}$  ETX2514 and monitored for the first 20 s. Data were linearized using a Dixon plot of inverse initial steady-state velocities ( $1/v_0$ ) versus inhibitor concentration ( $[I]$ ). The observed  $K_{i \text{ app}}$  was determined by dividing the value for the y-axis intercept by the slope of the line. The data were corrected to account for the substrate concentration and affinity for the  $\beta$ -lactamase using equation 1.

$$K_{i \text{ app}}(\text{corrected}) = K_{i \text{ app}}(\text{observed}) / (1 + [S] / [K_m \text{ substrate}]) \quad (1)$$

where  $[S]$  is the concentration of the substrate.

**$k_2/K_i$ .** Progress curves of  $\beta$ -lactamases mixed with increasing concentrations of ETX2514 using 100  $\mu\text{M}$  NCF (OXA-58 and ADC-7) (85  $\mu\text{M}$  NCF for OXA-58) or 300  $\mu\text{M}$  imipenem (OXA-66) as a reporter substrate were fit to equation 2 to obtain  $k_{\text{obs}}$  values.

**TABLE 8** Data collection and refinement statistics for ETX2514 complex with OXA-24/40

Data collection	OXA-24/40 + ETX2514
Wavelength (Å)	0.97946
Data range (outer shell) (Å)	1.95–37.3 (1.95–2.0)
Space group	P4 <sub>1</sub> 2 <sub>1</sub> 2
Cell dimensions (Å)	102.6 102.6 87.0 90° 90° 90°
Completeness (outer shell) (%)	99.6 (99.3)
Unique reflections (outer shell)	34,248 (2,350)
Total no. of observations (outer shell)	226,430
Average multiplicity (outer shell)	6.6 (6.5)
Mean I/sd(I) (outer shell)	11.3 (2.4)
R <sub>merge</sub> (%)	10.5 (79.1)
Refinement	
Resolution (Å)	1.95–37.3
R <sub>work</sub>	0.187
R <sub>free</sub>	0.210
No. of molecules (a.s.u.)	1
Ligands	1 ETX2514, 1 Cl
No. of water molecules	192
RMSD bond length (Å)	0.012
RMSD bond angles (°)	1.51

$$y = V_f x + (V_0 - V_f) [1 - \exp(-k_{\text{obs}} x)] / k_{\text{obs}} + A_0 \quad (2)$$

where  $V_0$  is the initial velocity,  $V_f$  is the final velocity, and  $A_0$  is the initial absorbance.

The  $k_{\text{obs}}$  data were plotted against the concentration of ETX2514. The acylation rate was obtained by correcting the value obtained for the slope of the line ( $k_2/K_i$ ) for the use of the reporter substrate (NCF or imipenem [IMI]) (equation 3).

$$k_2/k_i = k_2 k_i \{ ([S]/K_m \text{NCF or IMI}) + 1 \} \quad (3)$$

**$k_{\text{cat}}/k_{\text{inact}}$ .** Partition ratios at 24 h for ADC-7 and OXA-58 with ETX2514 were obtained by incubating each  $\beta$ -lactamase with increasing concentrations of ETX2514. The ratio of inhibitor to enzyme (I:E) necessary to inhibit the hydrolysis of NCF by >95% was determined.

**$k_{\text{off}}$ .** To determine the off-rate of ETX2514 for ADC-7, the  $\beta$ -lactamase (1  $\mu\text{M}$ ) was incubated with 825 nM ETX2514 for 5 min, diluted 1:10,000, and reacted with 100  $\mu\text{M}$  NCF. OXA-58  $\beta$ -lactamase (1  $\mu\text{M}$ ) was incubated with 2.9  $\mu\text{M}$  ETX2514 for 5 min, diluted 1:1,000, and reacted with 85  $\mu\text{M}$  NCF. Progress curves of NCF hydrolysis were collected for 1 h, and the data were fit to a single exponential decay equation to obtain  $k_{\text{off}}$ .  $\beta$ -lactamase alone and ETX2514 alone were used as controls.

**Electrospray ionization mass spectrometry of  $\beta$ -lactamases.** To discern the nature of the intermediates of inactivation by ETX2514 in the reaction pathway with  $\beta$ -lactamases, electrospray ionization (ESI) mass spectrometry (MS) was performed on a Waters Synapt G2-Si quadrupole-time-of-flight mass spectrometer. The Synapt G2-Si mass spectrometer was calibrated with a sodium iodide solution using a mass range of 50 to 2000  $m/z$ . Five micrograms of each  $\beta$ -lactamase (ADC-7 and OXA-58) were incubated with ETX2514 at a 1:1 molar ratio for 5 min, 30 min, or 24 h at room temperature in 10 mM phosphate-buffered saline (PBS), pH 7.4. Reactions were quenched with the addition of 0.1% formic acid in water and 1% acetonitrile. The samples were analyzed using Q-TOF coupled to a Waters Acquity H class ultraperformance liquid chromatograph (UPLC) with an Acquity UPLC BEH C<sub>18</sub> column (1.7  $\mu\text{m}$ ; 2.1 by 100 mm). The mobile phase consisted of 0.1% formic acid in water. The  $\beta$ -lactamase and  $\beta$ -lactamase-ETX2514 complexes were eluted using a gradient with final conditions of 15% mobile phase and 85% organic phase (100% acetonitrile with 0.1% formic acid). The tune settings for each of the data run was as follows: capillary voltage at 3.5 kV, sampling cone at 35, source offset at 35, source temperature at 100°C, desolvation temperature at 500°C, cone gas at 100 liters/h, desolvation gas at 800 liters/h, and nebulizer bar at 6.0. The protein peaks were deconvoluted using the MaxEnt1 program in MassLynx v4.1 software.

**OXA-58 acyl-transfer experiment.** To characterize the acyl transfer, the OXA-58  $\beta$ -lactamase (10  $\mu\text{M}$ ) was incubated with 10  $\mu\text{M}$  ETX2514 for 1 min. Immediately thereafter, the ability of the acylated OXA-58 to donate the acyl group to a second recipient  $\beta$ -lactamase was tested by the addition of a 10  $\mu\text{M}$  concentration of the class A KPC-2  $\beta$ -lactamase. The  $k_{\text{off}}$  and  $k_2/K_i$  of KPC-2 were reported previously as  $1.0 \pm 0.1 \times 10^{-3} \text{ s}^{-1}$  (1) and  $(9.3 \pm 0.6 \times 10^5 \text{ M}^{-1} \text{ s}^{-1})$  (2). The dual  $\beta$ -lactamase reaction was terminated after 15 s, 1 min, 30 min, 1 h, 2 h, 18 h, and 24 h and prepared for mass spectrometry as described above.

**Preparation of whole-genome DNA from *A. baumannii* isolates.** The genomic DNA from four *A. baumannii* isolates (AB052, AB053, AB054, and AB070) with sulbactam ETX2514 MICs of  $\geq 8 \text{ mg/liter}$  was isolated using the MasterPure Gram-positive DNA purification kit (Epicentre). Whole-genome sequencing was performed as previously described (31).

**Cocrystallization of OXA-24/40 with ETX2514.** The OXA-24/40  $\beta$ -lactamase (5  $\mu\text{M}$ ) was incubated with ETX2514 compound (250  $\mu\text{M}$ ) in 10 mM Tris-HCl (pH 7.8) buffer at 4°C overnight. Subsequently, this reaction mixture was purified over a Superdex 75 size exclusion column in buffer containing 10 mM Tris-HCl (pH 7.8) and 0.15 mM ETX2514. The eluted protein was concentrated to 7 mg/ml and crystallized

using the Classic Suite crystallization screening kit (Qiagen) with a 1:1 ratio of protein to reservoir solution in the drop. Best crystals were obtained in a crystallization condition consisting of 0.1 M HEPES sodium salt (pH 7.5), 10% (vol/vol) isopropanol, and 20% (wt/vol) PEG 4000. Crystals were frozen after 3 days of setting up the crystallization experiments.

**X-ray data collection and refinement.** Data for the ETX2514–OXA-24/40 complex were collected at the SSRL beamline and processed using AutoXDS scripts (32, 33) (Table 8). The  $\beta$ -lactamase structure was refined using the Refmac (34) and Coot programs (35). The starting protein coordinates for the OXA-24/40 starting structure was PDB identifier (ID) 3mbz. The parameter and topology files for ETX2514 were generated using the PRODRG program (36). The coordinates were checked using the structure validation program PROCHECK (37) and found to have no outliers in the Ramachandran plot. Coordinates and structure factors of the OXA-24–ETX2514 complex have been deposited in Protein Data Bank (PDB ID 6MPQ).

**Murine thigh infection model.** All animal procedures were performed at Neosome LLC under the supervision of an IACUC utilizing policies consistent with OLAW standards for the ethical treatment and welfare of animals. Following 5 days of acclimation to the facility, Crl:CD-1 mice ( $n = 3$ /treatment group) were rendered transiently neutropenic via two doses of cyclophosphamide administered intraperitoneally on days  $-4$  and  $-1$  at doses of 150 mg/kg and 100 mg/kg, respectively. Following overnight plate culture, some of the bacterial colonies were resuspended in sterile saline and adjusted to deliver  $1.0 \times 10^7$  CFU/mouse into each thigh of mice via intramuscular injection (100  $\mu$ l). At 2 h following inoculation, mice were dosed subcutaneously q3h separately with vehicle (control), ETX2514, sulbactam, and combinations of ETX2514 and sulbactam. Colistin was also administered to a separate group of animals at 40 mg/kg q24h as a positive therapy control. Animals were euthanized 24 h after the initiation of therapy, thighs were excised aseptically, weighed, and homogenized in 2 ml of sterile saline. Homogenates were then serially diluted, plated on growth media, and incubated overnight at 37°C, and CFU were enumerated the following day. Bacterial burden was expressed as  $\log_{10}$  CFU/g of tissue, and the change in burden over the 24-h course of therapy was considered as a measure of efficacy.

## ACKNOWLEDGMENTS

Research reported in this publication was supported in part by a research grant from Entasis Therapeutics (R.A.B. and F.V.D.A.), by funds and/or facilities provided by the Cleveland Department of Veterans Affairs to K.M.P.-W. and R.A.B., the Veterans Affairs Merit Review Program Awards 1101BX002872 (K.M.P.-W.) and 1101BX001974 (R.A.B.) from the Biomedical Laboratory Research & Development Service of the VA Office of Research and Development, the Geriatric Research Education and Clinical Center VISN 10 (R.A.B.), and the National Institute of Allergy and Infectious Diseases of the National Institutes of Health under awards R01AI100560, R01AI063517, and R01AI072219 to R.A.B.

P.N.R. is supported by VA Merit Award I01 BX001725 and Research Career Scientist Award IK6BX004470, both from the Department of Veterans Affairs.

We thank Neosome Life Sciences for executing the *in vivo* efficacy studies.

The content is solely the responsibility of the authors and does not necessarily represent the official views of the National Institutes of Health, the U.S. Department of Veterans Affairs, or the U.S. Government.

## REFERENCES

- Shapiro AB, Gao N, Jahic H, Carter NM, Chen A, Miller AA. 2017. Reversibility of covalent, broad-spectrum serine  $\beta$ -lactamase inhibition by the diazabicyclooctenone ETX2514. *ACS Infect Dis* 3:833–844. <https://doi.org/10.1021/acsinfecdis.7b00113>.
- Durand-Reville TF, Guler S, Comita-Prevoir J, Chen B, Bifulco N, Huynh H, Lahiri S, Shapiro AB, McLeod SM, Carter NM, Moussa SH, Velez-Vega C, Olivier NB, McLaughlin R, Gao N, Thresher J, Palmer T, Andrews B, Giacobbe RA, Newman JV, Ehmann DE, de Jonge B, O'Donnell J, Mueller JP, Tommasi RA, Miller AA. 2017. ETX2514 is a broad-spectrum  $\beta$ -lactamase inhibitor for the treatment of drug-resistant Gram-negative bacteria including *Acinetobacter baumannii*. *Nat Microbiol* 2:17104. <https://doi.org/10.1038/nmicrobiol.2017.104>.
- Ehmann DE, Jahic H, Ross PL, Gu RF, Hu J, Kern G, Walkup GK, Fisher SL. 2012. Avibactam is a covalent, reversible, non- $\beta$ -lactam  $\beta$ -lactamase inhibitor. *Proc Natl Acad Sci U S A* 109:11663–11668. <https://doi.org/10.1073/pnas.1205073109>.
- Ehmann DE, Jahic H, Ross PL, Gu RF, Hu J, Durand-Reville TF, Lahiri S, Thresher J, Livchak S, Gao N, Palmer T, Walkup GK, Fisher SL. 2013. Kinetics of avibactam inhibition against Class A, C, and D  $\beta$ -lactamases. *J Biol Chem* 288:27960–27971. <https://doi.org/10.1074/jbc.M113.485979>.
- Blizzard TA, Chen H, Kim S, Wu J, Bodner R, Gude C, Imbriglio J, Young K, Park YW, Ogawa A, Raghoobar S, Hairston N, Painter RE, Wisniewski D, Scapin G, Fitzgerald P, Sharma N, Lu J, Ha S, Hermes J, Hammond ML. 2014. Discovery of MK-7655, a beta-lactamase inhibitor for combination with Primaxin<sup>®</sup>. *Bioorg Med Chem Lett* 24:780–785. <https://doi.org/10.1016/j.bmcl.2013.12.101>.
- Lapuebla A, Abdallah M, Olafisoye O, Cortes C, Urban C, Landman D, Quale J. 2015. Activity of imipenem with relebactam against Gram-negative pathogens from New York City. *Antimicrob Agents Chemother* 59:5029–5031. <https://doi.org/10.1128/AAC.00830-15>.
- Haidar G, Clancy CJ, Chen L, Samanta P, Shields RK, Kreiswirth BN, Nguyen MH. 2017. Identifying spectra of activity and therapeutic niches for ceftazidime-avibactam and imipenem-relebactam against carbapenem-resistant Enterobacteriaceae. *Antimicrob Agents Chemother* 61:e00642-17. <https://doi.org/10.1128/AAC.00642-17>.
- Moya B, Barcelo IM, Bhagwat S, Patel M, Bou G, Papp-Wallace KM, Bonomo RA, Oliver A. 2017. WCK 5107 (Zidebactam) and WCK 5153 are novel inhibitors of PBP2 showing potent " $\beta$ -lactam enhancer" activity against *Pseudomonas aeruginosa*, including multidrug-resistant metallo- $\beta$ -lactamase-producing high-risk clones. *Antimicrob Agents Chemother* 61:e02529-16. <https://doi.org/10.1128/AAC.02529-16>.

9. Mushtaq S, Warner M, Livermore DM. 2010. *In vitro* activity of ceftazidime+NXL104 against *Pseudomonas aeruginosa* and other non-fermenters. *J Antimicrob Chemother* 65:2376–2381. <https://doi.org/10.1093/jac/dkq306>.
10. Shapiro A, Guler S, Carter N, Comita-Prevoir J, McLeod S, deJonge B, McLaughlin R, Huynh H, Gao N, Prince D, Ferguson A, Velez C, Durand-Réville T, Miller A, Mueller J, Tommasi R. 2016. ETX2514, a novel, rationally designed inhibitor of class A, C and D  $\beta$ -lactamases, for the treatment of Gram-negative infections, abstr LB-024. *ASM Microbe 2016*, Boston, MA. American Society for Microbiology, Washington, DC.
11. O'Donnell J, Newman J, Tanudra A, Chen A, De Jonge B, Shankaran H, Mueller J, Tommasi R. 2016. In vitro and in vivo efficacy of the novel  $\beta$ -lactamase inhibitor ETX2514 combined with sulbactam against multidrug resistant *Acinetobacter baumannii*, abstr LB-117. *ASM Microbe 2016*, Boston, MA. American Society for Microbiology, Washington, DC.
12. Nowak P, Paluchowska P. 2016. *Acinetobacter baumannii*: biology and drug resistance - role of carbapenemases. *Folia Histochem Cytobiol* 54:61–74. <https://doi.org/10.5603/FHC.a2016.0009>.
13. Evans BA, Amyes SG. 2014. OXA beta-lactamases. *Clin Microbiol Rev* 27:241–263. <https://doi.org/10.1128/CMR.00117-13>.
14. Hujer KM, Hujer AM, Hulten EA, Bajaksouzian S, Adams JM, Donskey CJ, Ecker DJ, Massire C, Eshoo MW, Sampath R, Thomson JM, Rather PN, Craft DW, Fishbain JT, Ewell AJ, Jacobs MR, Paterson DL, Bonomo RA. 2006. Analysis of antibiotic resistance genes in multidrug-resistant *Acinetobacter* sp. isolates from military and civilian patients treated at the Walter Reed Army Medical Center. *Antimicrob Agents Chemother* 50:4114–4123. <https://doi.org/10.1128/AAC.00778-06>.
15. Clinical and Laboratory Standards Institute. 2017. Performance standards for antimicrobial susceptibility testing; twenty-seventh informational supplement. *Clinical and Laboratory Standards Institute*, Wayne, PA.
16. Corbella X, Ariza J, Ardanuy C, Vuelta M, Tubau F, Sora M, Pujol M, Gudiol F. 1998. Efficacy of sulbactam alone and in combination with ampicillin in nosocomial infections caused by multiresistant *Acinetobacter baumannii*. *J Antimicrob Chemother* 42:793–802. <https://doi.org/10.1093/jac/42.6.793>.
17. McLeod SM, Shapiro AB, Moussa SH, Johnstone M, McLaughlin RE, de Jonge BLM, Miller AA. 2018. Frequency and mechanism of spontaneous resistance to sulbactam combined with the novel beta-lactamase inhibitor ETX2514 in clinical isolates of *Acinetobacter baumannii*. *Antimicrob Agents Chemother* 62:e01576-17. <https://doi.org/10.1128/AAC.01576-17>.
18. Cayó R, Rodríguez M-C, Espinal P, Fernández-Cuenca F, Ocampo-Sosa AA, Pascual A, Ayala JA, Vila J, Martínez-Martínez L. 2011. Analysis of genes encoding penicillin-binding proteins in clinical isolates of *Acinetobacter baumannii*. *Antimicrob Agents Chemother* 55:5907–5913. <https://doi.org/10.1128/AAC.00459-11>.
19. Carruthers MD, Harding CM, Baker BD, Bonomo RA, Hujer KM, Rather PN, Munson RS, Jr. 2013. Draft genome sequence of the clinical isolate *Acinetobacter nosocomialis* strain M2. *Genome Announc* 1:e00906-13. <https://doi.org/10.1128/genomeA.00906-13>.
20. Yoon EJ, Courvalin P, Grillot-Courvalin C. 2013. RND-type efflux pumps in multidrug-resistant clinical isolates of *Acinetobacter baumannii*: major role for AdeABC overexpression and AdeRS mutations. *Antimicrob Agents Chemother* 57:2989–2995. <https://doi.org/10.1128/AAC.02556-12>.
21. Magnet S, Courvalin P, Lambert T. 2001. Resistance-nodulation-cell division-type efflux pump involved in aminoglycoside resistance in *Acinetobacter baumannii* strain BM4454. *Antimicrob Agents Chemother* 45:3375–3380. <https://doi.org/10.1128/AAC.45.12.3375-3380.2001>.
22. Marchand I, Damier-Piolle L, Courvalin P, Lambert T. 2004. Expression of the RND-type efflux pump AdeABC in *Acinetobacter baumannii* is regulated by the AdeRS two-component system. *Antimicrob Agents Chemother* 48:3298–3304. <https://doi.org/10.1128/AAC.48.9.3298-3304.2004>.
23. Coyne S, Courvalin P, Perichon B. 2011. Efflux-mediated antibiotic resistance in *Acinetobacter* spp. *Antimicrob Agents Chemother* 55:947–953. <https://doi.org/10.1128/AAC.01388-10>.
24. Shapiro A, Moussa S, Tommasi R, Mueller J, O'Donnell J, Miller A. 2017. Restoration of sulbactam activity against multidrug-resistant *Acinetobacter baumannii* by the novel, broad spectrum beta-lactamase inhibitor ETX2514 correlates with beta-lactamase inhibition in vitro and in vivo. OS0562. 27th ECCMID, Vienna, Austria. European Society of Clinical Microbiology and Infectious Diseases, Basel, Switzerland.
25. Barnes MD, Winkler ML, Taracila MA, Page MGP, Desarbre E, Kreiswirth BN, Shields RK, Nguyen MH, Clancy CJ, Spellberg B, Papp-Wallace KM, Bonomo RA. 2017. *Klebsiella pneumoniae* carbapenemase-2 (KPC-2), substitutions at Ambler position Asp179, and resistance to ceftazidime-avibactam: unique antibiotic-resistant phenotypes emerge from  $\beta$ -lactamase protein engineering. *mBio* 8:e00528-17. <https://doi.org/10.1128/mBio.00528-17>.
26. Che T, Bethel CR, Pusztai-Carey M, Bonomo RA, Carey PR. 2014. The different inhibition mechanisms of OXA-1 and OXA-24 beta-lactamases are determined by the stability of active site carboxylated lysine. *J Biol Chem* 289:6152–6164. <https://doi.org/10.1074/jbc.M113.533562>.
27. Papp-Wallace KM, Nguyen NQ, Jacobs MR, Bethel CR, Barnes MD, Kumar V, Bajaksouzian S, Rudin SD, Rather PN, Bhavsar S, Ravikumar T, Deshpande PK, Patil V, Yeole R, Bhagwat SS, Patel MV, van den Akker F, Bonomo RA. 2018. Strategic approaches to overcome resistance against Gram-negative pathogens using beta-lactamase inhibitors and beta-lactam enhancers: activity of three novel diazabicyclooctanes, WCK 5153, zidebactam (WCK 5107), and WCK 4234. *J Med Chem* 61:4067–4086. <https://doi.org/10.1021/acs.jmedchem.8b00091>.
28. Shapiro AB. 2017. Kinetics of sulbactam hydrolysis by beta-lactamases, and kinetics of beta-lactamase inhibition by sulbactam. *Antimicrob Agents Chemother* 61:e01612-17. <https://doi.org/10.1128/AAC.01612-17>.
29. Morrison JF, Walsh CT. 1988. The behavior and significance of slow-binding enzyme inhibitors. *Adv Enzymol Relat Areas Mol Biol* 61:201–301.
30. Papp-Wallace KM, Winkler ML, Gatta JA, Taracila MA, Chilakala S, Xu Y, Johnson JK, Bonomo RA. 2014. Reclaiming the efficacy of  $\beta$ -lactam- $\beta$ -lactamase inhibitor combinations: avibactam restores the susceptibility of CMY-2-producing *Escherichia coli* to ceftazidime. *Antimicrob Agents Chemother* 58:4290–4297. <https://doi.org/10.1128/AAC.02625-14>.
31. Penwell WF, Shapiro AB, Giacobbe RA, Gu RF, Gao N, Thresher J, McLaughlin RE, Huband MD, DeJonge BL, Ehmann DE, Miller AA. 2015. Molecular mechanisms of sulbactam antibacterial activity and resistance determinants in *Acinetobacter baumannii*. *Antimicrob Agents Chemother* 59:1680–1689. <https://doi.org/10.1128/AAC.04808-14>.
32. Gonzalez A, Tsay Y. 2010. A quick XDS tutorial for SSRL. <http://smb.slac.stanford.edu/facilities/software/xds/>.
33. Kabsch W. 2010. Xds. *Acta Crystallogr D Biol Crystallogr* 66:125–132. <https://doi.org/10.1107/S0907444909047337>.
34. Murshudov GN, Vagin AA, Dodson EJ. 1997. Refinement of macromolecular structures by the maximum-likelihood method. *Acta Crystallogr D Biol Crystallogr* 53:240–255. <https://doi.org/10.1107/S0907444996012255>.
35. Emsley P, Cowtan K. 2004. Coot: model-building tools for molecular graphics. *Acta Crystallogr D Biol Crystallogr* 60:2126–2132. <https://doi.org/10.1107/S0907444904019158>.
36. Schuttelkopf AW, van Aalten DM. 2004. PRODRG: a tool for high-throughput crystallography of protein-ligand complexes. *Acta Crystallogr D Biol Crystallogr* 60:1355–1363. <https://doi.org/10.1107/S0907444904011679>.
37. Laskowski RA, MacArthur MW, Moss DS, Thornton JM. 2001. PROCHECK - a program to check the stereochemical quality of protein structures. *J Appl Crystallogr* 26:283–291. <https://doi.org/10.1107/S0021889892009944>.
38. Lahiri SD, Mangani S, Jahic H, Benvenuti M, Durand-Reville TF, De Luca F, Ehmann DE, Rossolini GM, Alm RA, Docquier JD. 2015. Molecular basis of selective inhibition and slow reversibility of avibactam against class D carbapenemases: a structure-guided study of OXA-24 and OXA-48. *ACS Chem Biol* 10:591–600. <https://doi.org/10.1021/cb500703p>.